JOURNAL OF AGRICULTURAL AND FOOD CHEMISTRY

Rapid Measurement and Evaluation of the Effect of Drying Conditions on Harpagoside Content in *Harpagophytum procumbens* (Devil's Claw) Root

ELIZABETH JOUBERT,*,† MARENA MANLEY,*,‡ BRIAN R. GRAY,‡ AND HARTWIG SCHULZ§

ARC Infruitec-Nietvoorbij, Private Bag X5026, Stellenbosch, 7599, South Africa, Department of Food Science, Stellenbosch University, Private Bag X1, Matieland (Stellenbosch), 7602, South Africa, and Institute for Plant Analysis, Federal Centre for Breeding Research on Cultivated Plants (BAZ), Neuer Weg 22-23, 06484 Quedlinburg, Germany

The effect of drying conditions on harpagoside (HS) retention, as well as the use of near-infrared spectroscopy (NIRS) for rapid quantification of the iridoids, HS, and 8-*ρ*-coumaroyl harpagide (8*ρ*CHG) and moisture, in dried *Harpagophytum procumbens* (devil's claw) root was investigated. HS retention was significantly ($P < 0.05$) lower in sun-dried samples as compared to tunnel-dried (60 °C, 30% relative humidity) and freeze-dried samples. The best retention of HS was obtained at 50 °C when evaluating tunnel drying at dry bulb temperatures of 40, 50, and 60 °C and 30% relative humidity. NIRS can effectively predict moisture content with a standard error of prediction (SEP) and correlation coefficient (r) of 0.24% and 0.99, respectively. The HS and 8*ρ*CHG NIRS calibration models established for both iridoid glucosides can be used for screening purposes to get a semiquantitative classification of devil's claw roots (for HS: SEP = 0.236%, $r = 0.64$; for 8*ρ*CHG: SEP = 0.048%, $r = 0.73$).

KEYWORDS: ***Harpagophytum procumbens*; devil's claw; harpagoside; 8-*ρ*-coumaroyl harpagide; controlled drying; moisture content; NIRS; HPLC**

INTRODUCTION

Harpagophytum procumbens, commonly known as devil's claw, is a prostrate, perennial herb, indigenous to Southern Africa (*1*). The tuberous secondary roots are purported to possess antiinflammatory and analgesic activities (*1*−*3*). An infusion, prepared from powdered, dried root, is used against a range of ailments, including inflammation, headaches, rheumatism, and indigestion (*3*, *4*). The powdered tubers can be used either directly in a tea infusion or as pills produced by pharmaceutical companies. It has been suggested that a second species, *Harpagophytum zeyheri*, shows similar activities (*3*, *5*). Although both species have similar chemical compositions, *H. procumbens* has traditionally been preferred and many authors contend that this species exclusively has medicinal value (*3*, *6*, *7*).

The medicinal value is attributed to compounds of the iridoid family (*8*, *9*). Compounds of interest are the iridoid glucosides, i.e., harpagoside (HS) and 8-*ρ*-coumaroyl harpagide (8*ρ*CHG), which are concentrated in the secondary rhizoidal roots (*3*, *4*, *8*). Typically, HS is present in higher concentrations (ca. 2.0%) than 8*ρ*CHG (ca. 0.06%) in dried roots of *H. procumbens* (*3*, *6*). HS concentrations vary from 0.7 to 3.0% (*3*, *6*), and 8*ρ*CHG concentrations vary from 0.03 to 0.13% (*6*).

Poukens-Renwart et al. (*10*) suggested that a suitable minimum level of 1.2% HS should be enforced for standardization of the roots, as stipulated in both the Swiss Pharmacopoeia and Pharmeuropa. Usually, high-performance liquid chromatography (HPLC) analyses are used to determine the iridoid content of the root (*8*, *11*). However, for quality control, a rapid, yet still accurate, method is needed to ensure that dried root contains specified minimum levels of HS.

If the level of the measured analyte is sufficient, quantitative analyses by near-infrared spectroscopy (NIRS) may be successfully achieved (*12*−*14*). Baranska et al. (*15*) used NIR-FT-Raman spectroscopy to characterize distribution and quantify HS in secondary roots of *H. procumbens*. NIRS analyses of hypericin in *Hypericum perforatum* (St. John's Wort) extracts (*16*), ginsenosides in *Panax quinquefolium* (American ginseng) extracts (*12*), and polyphenols and alkaloids in *Camellia sinensis* (green tea) (*13*) have been performed successfully.

The roots are harvested by hand, sliced, and then typically sun-dried and exported without further processing. The final moisture content of the exported dried root is not regulated, but 10% or less is recommended to prevent microbial spoilage. Very little information is available on the stability of the major active compound, HS. Burger (*17*) linked the formation of blue−black discoloration in the cortical zone, during drying, to

* To whom correspondence should be addressed. (E.J.) Tel: +27 21 809 3444. Fax: +27 21 809 3400. E-mail: joubertl@arc.agric.za. (M.M.) Tel: +27 21 808 3511. Fax: +27 21 808 3511. E-mail: mman@sun.ac.za.
† ARC Infruitec-Nietvoorbij.
‡ Stellenbosch University.
§ Federal Centre for Breeding Research on Cultivated Plants (BAZ).

10.1021/jf047930c CCC: $30.25 © 2005 American Chemical Society
Published on Web 04/06/2005

polymerization reactions or acid lability of the aglycone moiety of HS. Because discoloration takes place during sun drying, it is possible that degradation of HS occurs. The extent of HS degradation would depend on climatic conditions, creating a need for controlled drying to obtain a more constant and higher quality product.

This study evaluated the relative effect that three drying methods (sun, tunnel, and freeze drying) and tunnel drying temperature (40, 50, and 60 °C) had on the HS content of devil's claw. The ability of NIRS to predict the HS, 8*ρ*CHG, and moisture contents in dried, ground *H. procumbens* root was also investigated.

MATERIALS AND METHODS

Preparation of Samples. Fresh *H. procumbens* secondary roots from cultivated plants were obtained in three batches from Grassroots Natural Products (Plant Improvement Centre, Gouda, South Africa). Before they were sliced, the roots were rinsed with tap water to remove the dirt. The roots were sliced transversely into 6 mm thick disks (Rheninghaus polony cutter, Italy), which were then cut into three triangular sectors of approximately the same size. The three sectors were randomly divided between the three drying treatments to minimize influences from any inter- and intraroot HS variation. Additional samples for development of NIRS prediction models were prepared from individual roots [sliced and tunnel-dried at 60 °C at 30% relative humidity (RH) for 24 h].

The dried samples were vacuum-sealed (Geiger & Klotzbücher Multivac, South Africa) in aluminum-laminated pouches to avoid any moisture uptake after drying and before grinding. Grinding of the samples was accomplished using a Retsch rotary mill fitted with a 1 mm sieve size. The ground samples were stored in 30 mL plastic screw cap vials and sealed in large plastic containers with anhydrous $CaCl_2$ as desiccant until analysis.

Drying Conditions. For sun drying, the samples were spread directly after slicing onto wooden drying trays (890 mm × 600 mm), and covered with a high-density polyethylene (HDPE) net (2 mm mesh, Netlon, Tensar International, United Kingdom). A second net was placed on top of the samples and weighed down with bricks to avoid dried samples being blown away. These trays were placed daily on a tarred drying court from 08:00 to 16:30 and then removed to a shed where a fan provided additional air movement during the night. Samples were considered dry when brittle. Weather data were obtained from the automatic weather station at the Nietvoorbij experimental farm (ARC Infruitec-Nietvoorbij, Stellenbosch, South Africa).

For comparison of the drying methods, ca. 450 g of fresh root was dried per sample, with eight replicates performed. A total of 24 individual samples (8 × 3 drying conditions) were therefore prepared. The conditions for tunnel drying were set at a dry bulb temperature (T_{DB}) of 60 °C and RH of 30%, i.e., a wet bulb temperature (T_{WB}) of 39.72 °C. A purpose-built experimental dehydrator was used for drying at an air velocity of 3 m/s. The system was computer-controlled with isothermal temperature control of both the T_{DB} and the T_{WB} values by CAL 3200 Autotune temperature modules (Ana-Digi Systems, Bellville, South Africa). The total drying time was fixed at 24 h.

Samples that were freeze-dried were initially frozen at −20 °C in plastic trays (170 mm × 115 mm × 30 mm). The frozen samples were then dried for 5 days in an Atlas pilot-scale freeze-drier (Denmark model, Copenhagen, Denmark) at a shelf temperature of 40 °C.

For comparison of the effect of drying temperature on the retention of HS during tunnel drying, the conditions at 30% RH were used as follows: T_{DB} of 40 °C (T_{WB} of 26.09 °C), T_{DB} of 50 °C (T_{WB} of 32.32 °C), and T_{DB} of 60 °C (T_{WB} of 39.72 °C). After they were sliced, the samples (ca. 450 g each) were immediately spread onto stainless steel mesh drying trays (870 mm × 600 mm), covered with an HDPE net, and dried. Three purpose-built experimental dehydrators, one controlled by the CAL 3200 Autotune temperature modules (Ana-Digi Systems) and the other two configured as described by Hansmann and Van Noort (*18*), were used. The air velocity of the last two driers was controlled at 4 m/s.

Nine replicates were performed per drying temperature, with the replicates balanced between the three drying tunnels to avoid intertunnel variation. A total of 27 individual samples (9 × 3 temperatures) were therefore prepared. To ensure that all samples were dried to approximately the same moisture content, different drying times for each temperature were used. Termination of tunnel drying was estimated from drying curves calculated after drying in a small-scale experimental dehydrator. Fresh devil's claw root (ca. 1.3 kg per sample) was spread on 30 mesh stainless steel trays (370 mm × 310 mm) and dried at 40, 50, and 60 °C, respectively. The trays were mounted in a cage, suspended from two single-point Tedea-Huntleigh 1040 load cells (Loadtech Ltd., Centurion, South Africa), the output of which was digitized using an Advantech Adam 4011 analogue input module (ProMicro cc., Bryanston, South Africa). Computerized data acquisition was achieved via an Adam 4520 RS-232/485 converter (ProMicro cc.) with changes in mass recorded at 2 min intervals.

Drying Rate Curves. Drying rate curves were generated from MS-Excel 2000 spreadsheets and approximated by polynomial least-squares fitting. The drying times were estimated from a plot of moisture content vs time. Once drying in larger tunnels with roots harvested at a later stage commenced, these times proved too short and were subsequently adjusted to 17 h for T_{DB} of 40 °C, 11 h for T_{DB} of 50 °C, and 6 h for T_{DB} of 60 °C.

Moisture Determination. The moisture content was determined gravimetrically in duplicate. The dried, ground sample was weighed into nickel moisture dishes before drying under vacuum (ca. 90 kPa) for 16 h at 70 °C.

Extraction of Iridoids. The relative extraction potential of 100% MeOH and 70% MeOH−H_2O was evaluated. A duplicate set of 12 dried, ground samples (ca. 0.15 g) was extracted, each with one of the solvents (15 mL), in sealed glass vials in a water bath at 40 °C for 60 min. The extracts were manually shaken at 15 min intervals, cooled to ambient temperature in tap water for 10−15 min, and centrifuged at 4000 r/min (1788.8*g*) for 12 min in a Universal 16 centrifuge (Hettich Zentrifugen, Germany). The supernatants were stored in glass vials with Teflon-lined screw caps at ca. 4 °C until analyzed. The samples obtained during drying experiments and development of the NIRS calibration model were extracted with the 70% MeOH−H_2O mixture.

HPLC Analysis. HPLC separations were carried out, in duplicate, using a Waters LC Module 1 plus system, equipped with a single wavelength UV−visible detector and controlled by Millennium workstation software (version 2.15, Waters Corporation, United Kingdom). The HPLC method of Feistel and Gaedcke (*11*) was followed after slight modifications; that is, the solvent program was lengthened from 60 to 70 min to allow better equilibration of the column with the aqueous phase before the next injection. Separations were carried out on a Phenomenex Prodigy 5 ODS-2 column (150 mm × 4.60 mm, 5 *μ*m particle size) equipped with a Jour-Guard RP/C18-5*μ* guard column at 40 °C and a flow rate of 0.7 mL/min. The solvent gradient consisted of water and methanol (HPLC grade, Chromasolv, Merck, Cape Town, South Africa), degassed in-line with a Jour Research X-ACT degasser. The column, guard column, and degasser were supplied by Separations (Cape Town, South Africa). Purified water (Modulab water purification system, Separations) was further treated with a Milli-Q Académic ultrapure water system (Millipore, Ireland) for HPLC use.

An aliquot of the extract supernatant was filtered through a 0.45 *μ*m HV type filter (13 mm, Millipore) before injection (10 *μ*L). Absorbance was measured at 278 or 312 nm for the detection of HS and 8*ρ*CHG, respectively (*8*, *11*). A dilution series of pure HS (Extrasynthese, Genay, France) for the development of a calibration curve (0.5−2.4 *μ*g/10 *μ*L) was prepared with HPLC grade methanol (Chromasolv, Merck). Two concentration ranges (0.049−0.323 and 0.388−2.425 *μ*g/10 *μ*L) were used for the quantification of 8*ρ*CHG. The pure standard was supplied by PhytoLab (Addipharma) (Hamburg, Germany).

Near Infrared Spectroscopy Measurements. The Perkin-Elmer Fourier transform near-infrared (FT-NIR) spectrophotometer, Spectrum IdentiCheck, fitted with the IdentiCheck Reflectance Accessory (ICRA), was used to collect near-infrared (NIR) reflectance spectra from all samples prepared during the duration of the study. Samples were presented to the instrument in 4 mL Chromacol borosilicate glass vials

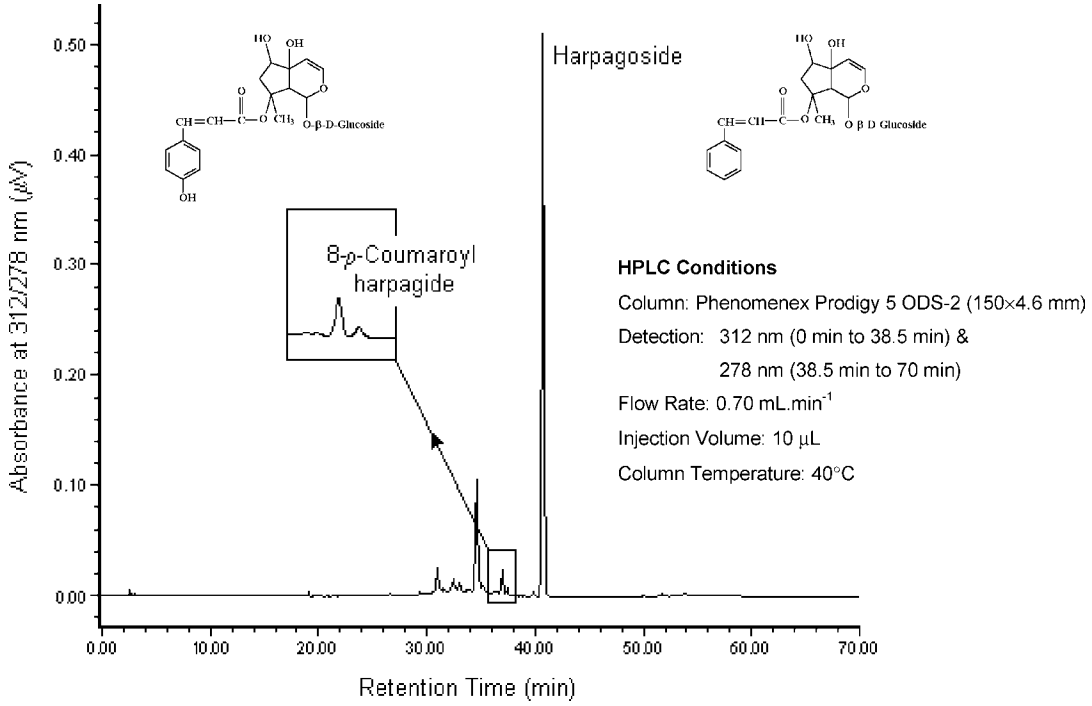

Figure 1. Typical HPLC chromatogram of *H. procumbens* extract (70% methanol–water) with program conditions and chemical structures of HS and 8ρCHG.

with screw caps. Spectra were measured (16 accumulations) from 10000 to 4000 cm^{-1} (1100−2500 nm) at a resolution of 16 cm^{-1}, resulting in 701 data points. Spectral measurements were converted from wavenumber to wavelength to be in accordance with current NIRS practice.

NIRS Calibration Development. Calibrations ($n = 100$) were developed (The Unscrambler version 6.11, CAMO ASA, Norway) for quantification of moisture, HS, and 8ρCHG contents using partial least squares (PLS) regression. Preprocessing of spectral data included multiplicative scatter correction (MSC), to eliminate variances caused by particle size differences, and Savitsky-Golay 1st derivatives to enhance slight spectral differences. The independent validation sets ($n = 50$) were selected to represent samples across the entire range of available reference values. Every third sample was chosen from ascending sorted references values of the complete data set ($n = 150$) with the samples with the highest and lowest reference values remaining in the calibration set.

Results were evaluated by means of the standard error of prediction (SEP). Either the SEP or the root-mean-square error of prediction (RMSEP), which both reflect the ability of a calibration to predict accurately and precisely the analyte values of the independent validation set (*19*), can be used. The SEP, however, is corrected for bias. The performances of the various calibrations were evaluated by comparison of the SEP to the corresponding standard error of laboratory (SEL) for the respective reference methods and evaluation of the RPD [ratio of standard deviation (SD) to SEP]. For any calibration, the aim is to reduce the SEP (or RMSEP) to approach the SEL of the reference method and for the RPD to be as large as possible.

Statistical Analyses. Statistical comparisons of data from drying experiments were preformed after analysis of variance, where replicates were treated as blocks, and Student's *t*-LSD test (least significance level = 0.05) was performed (SAS, version 6.12).

RESULTS AND DISCUSSION

Extraction of Iridoids. The large range of solvents used in other studies (*3*, *8*, *20*) for the extraction of HS in *H. procumbens* prompted the testing of two solvents with different polarities, i.e., 70% MeOH−H_2O and 100% MeOH. As the 70% MeOH−H_2O mixture resulted in significantly ($P < 0.05$) better extraction of HS, the method was standardized to use this mixture as solvent. A typical chromatogram of a *H. procumbens* extract is shown in **Figure 1**.

Table 1. Effect of Drying Method on Moisture and HS Contents of Devil's Claw Root

drying method	moisture	$HS_{drybasis}$	$HS_{drybasis}$ range
sun	6.17 ± 0.72 a[a]	1.455 ± 0.362 a	1.098–2.082
tunnel	3.43 ± 0.66 b	1.526 ± 0.396 b	1.149–2.198
freeze	5.08 ± 1.05 c	1.565 ± 0.394 b	1.169–2.170

[a] Values expressed as percentage are means ± SD. Values within the same column with different letters are significantly different ($P < 0.05$).

Drying Conditions. The freeze-dried samples retained the original shape of the root disks (little or no wrinkling) and the pale yellow color very similar to that of the fresh root. Both the sun- and the tunnel-dried samples shrunk and became twisted during drying. Light to dark brown discoloration occurred with the sun-dried samples having the darkest color. Some samples showed a greenish to blue−black discoloration in the cortical zone of the disks, indicative of possible polymerization or degradation reactions (*17*).

Sun drying required 3−5 days per sample, depending upon the prevalent weather conditions. The overall average temperatures (24 h) across all days ranged from 17.55 to 25.91 °C (mean ± SD: 21.82 ± 2.29 °C), with RH values varying between 53.11 and 81.31% (70.09 ± 9.58%). The sun-dried samples had the highest moisture content (6.17 ± 0.72%) of the different drying methods followed by the freeze-dried (5.08 ± 1.05%) and tunnel-dried (3.43 ± 0.66%) samples. The high moisture content of the sun-dried samples is attributed to the relatively low average drying temperatures, as compared to the higher tunnel temperatures. The larger the difference between ambient and drying temperatures, the larger the driving force for removing the water (*21*). A further factor was the much higher ambient RH values that would also have reduced the drying potential of this method. The respective average moisture and HS contents are given in **Table 1**.

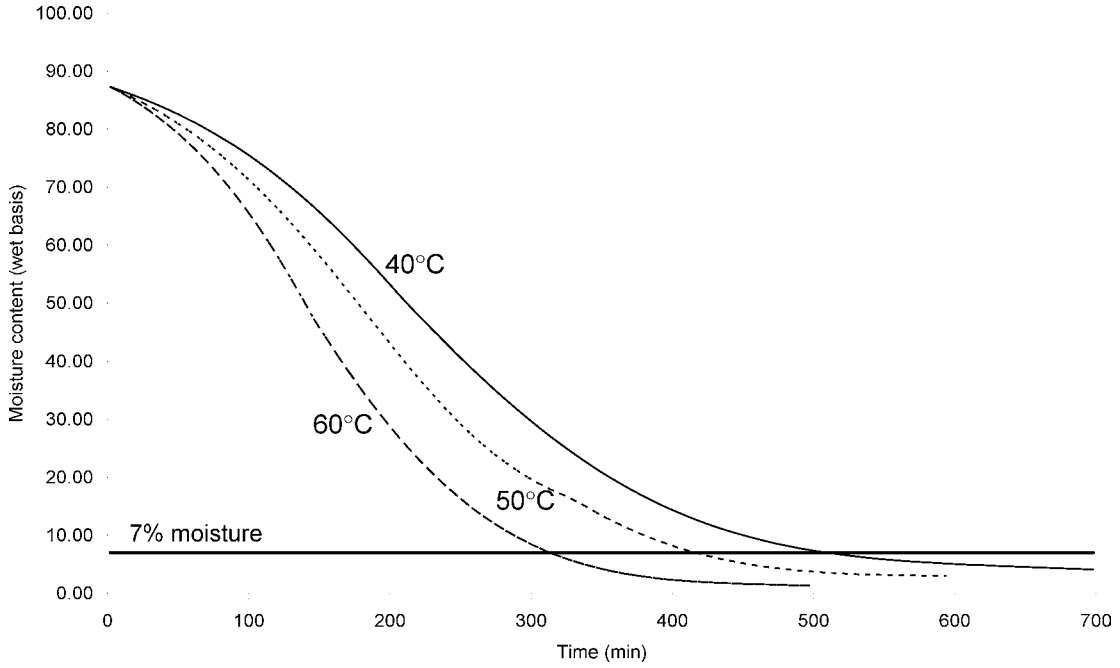

Figure 2. Percentage moisture content (wet basis) of devil's claw samples (6 mm disks), measured at three T_{DB} values, as a function of drying time.

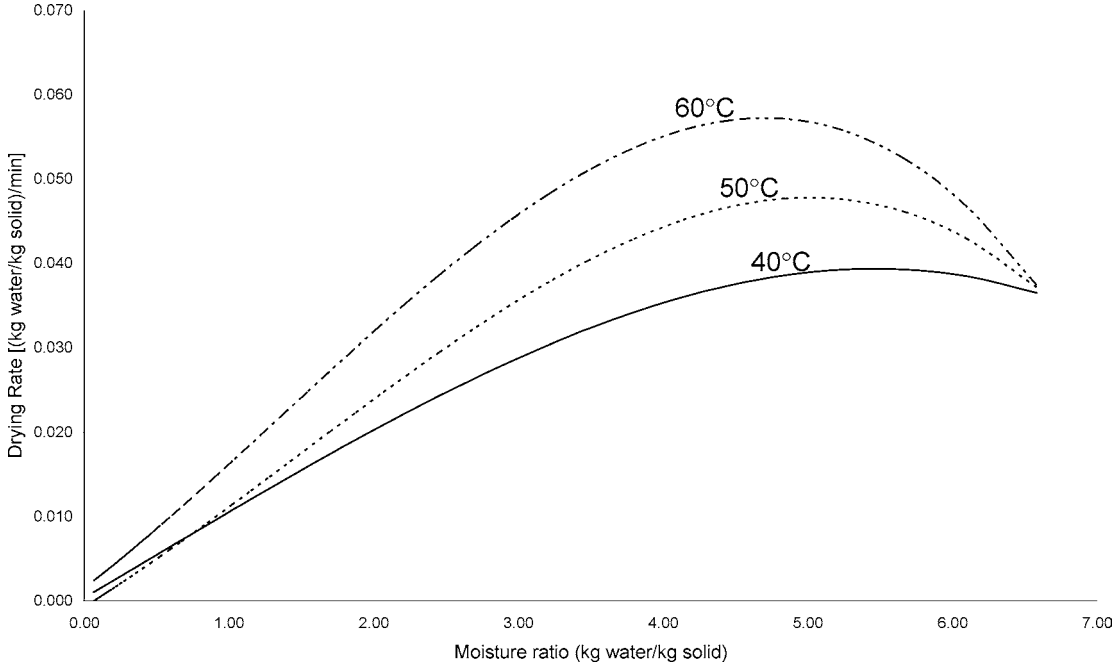

Figure 3. Drying rate of devil's claw samples, measured at three T_{DB} values, as a function of the moisture content (dry basis) during drying.

Sun drying resulted in significantly ($P < 0.05$) lower HS concentrations ($1.455 \pm 0.362\%$) as compared to the other two methods. The large SD reflects the relatively large HS range across the nine replicates (**Table 1**) that is indicative of the inter-root HS variation. It is assumed that the extent to which HS content decreased during sun drying is related to the duration of drying time. Slow drying, due to the high ambient RH values (ca. 70%), could have increased the incidence and degree of enzymatic degradation, by maintaining the water activity (a_w) above 0.7 for an extended period of time (*22*). Under these conditions, the initial stages of drying would be characterized by high levels of free water in the root, a prerequisite for enzymatic reactions. The ambient drying temperatures (average: 21.82 °C) would also be within the optimum range of many plant enzymes; especially polyphenol oxidase and glucosidases have been implicated in degrading reactions in plants (*23*, *24*).

As expected, freeze drying was the least detrimental drying technique because of the low drying temperature and the fact that reduced pressure caused the water component to change directly from a solid to a vapor phase (i.e., sublimation). The lack of extensive discoloration in the freeze-dried samples indicates that neither enzymatic nor nonenzymatic chemical reactions occurred. Operating a freeze drier for commercial drying purposes could, however, prove costly. Tunnel drying would be the preferred method, as an acceptable product (minimal decrease in HS content as compared to freeze drying; **Table 1**), at a lower cost, could be produced.

Table 2. Effect of Tunnel Drying Temperature on the Moisture and HS Contents of Dried, Ground Devil's Claw Root

temp (°C)	moisture	$HS_{as\ is}$[a]	HS_{DB}[b]
40	9.13 ± 1.16 a[c]	1.553 ± 0.389 a	1.710 ± 0.426 a
50	8.84 ± 1.00 a	1.597 ± 0.406 b	1.750 ± 0.438 b
60	8.71 ± 1.21 a	1.573 ± 0.410 ab	1.723 ± 0.444 ab

[a] $HS_{as\ is}$ = HS concentration (%) on a "moist mass" basis. [b] HS_{DB} = HS concentration (%) corrected for moisture (%, dry basis). [c] Values within the same column with different letters are significantly different ($P < 0.05$).

Table 3. Reference Data for Moisture, HS, and 8ρCHG Contents of Dried, Ground Devil's Claw Root

	moisture ($n = 150$)	$HS_{as\ is}$[a] ($n = 150$)	$8\rho CHG_{as\ is}$ ($n = 150$)
range (%)	2.44–10.43	0.693–2.244	0.027–0.310
mean (%)	4.47	1.348	0.152
SD	1.58	0.299	0.073
SEL[b]	0.14	0.035	0.010

[a] Ranges, means, and SDs for HS and 8pCHG are given on a moist mass ("as is") basis. [b] Reference method.

Drying Rate Curves. Drying curves were generated for the three tunnel drying temperatures, i.e., T_{DB} of 40, 50, and 60 °C at 30% RH. The main purpose of such curves is the modeling of the drier and the parameters of drying. This becomes important in the design of a drier, especially if product specific drying is required (*25*). One of the important drying parameters required for this study was the termination time that would produce samples of similar moisture content for each drying temperature.

Figure 2 shows the moisture content (wet basis) plotted against drying time at 40, 50, and 60 °C. The three curves were normalized by using an average ($n = 18$) solids content of 12.73%. From **Figure 2**, drying times required to produce products of ca. 7% moisture content can easily be estimated. At this moisture content, microbial spoilage and overdrying will be prevented. Commercially, overdrying would be undesirable from a production point of view as additional costs would be incurred with a prolonged drying period.

Initially, the calculated drying times were ca. 9, 7, and 5 h for 40, 50, and 60 °C, respectively. Roots harvested at a later stage required longer drying times, i.e., 17, 11, and 6 h each at the respective temperatures, even though the air velocity was slightly higher. It is possible that changes in the cellular structure of the roots, due to seasonal influences, could have increased the water-binding capacity of the samples. Stachyose, a tetrasaccharide, which would affect water-binding capacity, is abundant in the root with up to 46% occurring in dried material (*26*).

A plot of the drying rate of a sample as a function of its moisture content is depicted in **Figure 3**. Two drying rate periods are clearly visible on the plot, namely, induction, characterized by an increase in sample temperature, approaching T_{WB}, and the falling rate period. No clear constant rate period was obtained, indicating that the air velocity in the drying tunnel (2 m/s), the relatively large temperature differentials at constant 30% RH, i.e., 13.91 °C for T_{DB} of 40 °C, 17.68 °C for T_{DB} of 50 °C, and 20.28 °C for T_{DB} of 60 °C, and the relatively large surface area of the samples resulted in an evaporation rate higher than the rate of mass transfer.

Even though no clearly discernible constant rate drying was observed for any of the temperatures, drying at 40 °C provided the closest approximation to this period. Mild temperatures and a high free water content during this period of drying are ideal for possible enzyme reactions to occur (*21*). It was, therefore, desirable not to have an extended constant rate drying period, since enzymatic reactions during this period could possibly have a negative impact on the HS content of the root.

The falling rate periods of all three temperatures approximated a linear curve between moisture contents of ca. 0.5−3.5 kg water/kg solids. This linear decline indicates that no sudden changes, such as case hardening that would have been characterized by a decrease in the drying rate, occurred in the sample matrix (*27*, *28*).

Comparison of Drying Temperature. Temperature significantly ($P < 0.05$) affects the HS content (**Table 2**) with drying at 50 °C, the most beneficial for the retention of HS, suggesting that the evaporation and mass transfer of water from samples at this temperature were rapid enough to reduce the incidence

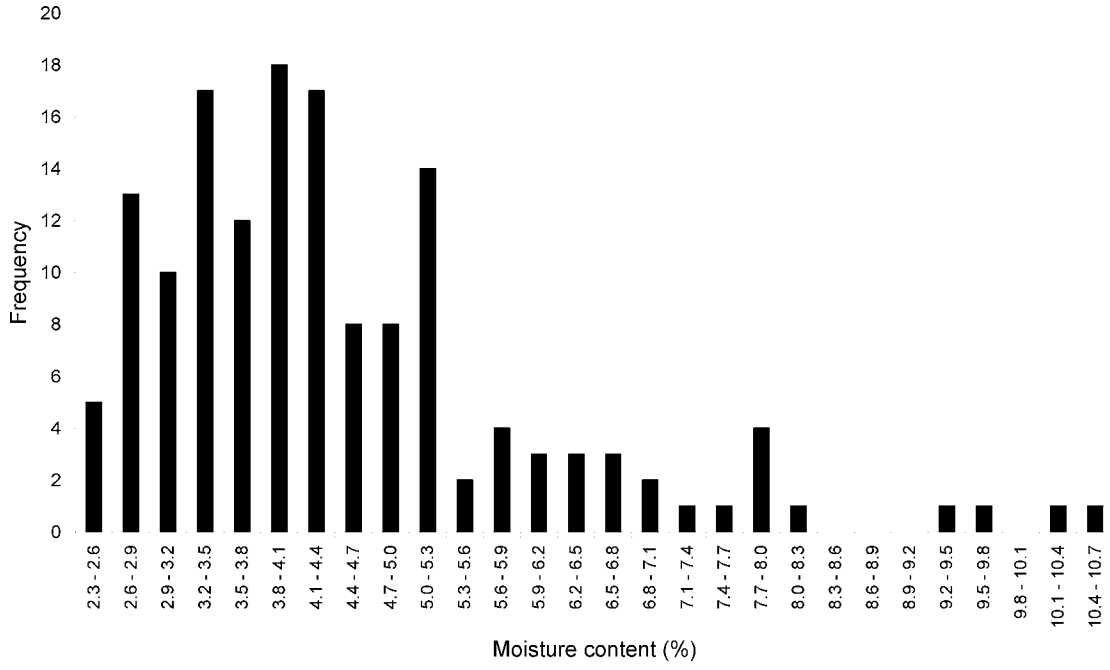

Figure 4. Histogram of the distribution of moisture content between samples of dried, ground devil's claw root ($n = 150$).

Table 4. Prediction Results for the Independently Validated Moisture, HS, and 8ρCHG Content FT-NIR Calibrations of Dried, Ground Devil's Claw Root

	moisture ($n = 150$)		$HS_{as\ is}$ ($n = 150$)		$8\rho CHG_{as\ is}$ ($n = 150$)	
	calibration set	validation set	calibration set	validation set	calibration set	validation set
range (%)	2.53–10.43	2.44–9.60	0.803–2.244	0.693–2.129	0.027–0.310	0.033–0.303
mean (%)	4.50	4.40	1.354	1.337	0.152	0.151
n[a]	100	50	100	50	100	50
SEP[b] (%)	0.24	0.236	0.048			
bias	0.01	–0.048	0.002			
r[c]	0.988	0.641	0.731			
PLS factors[d]	4	7	5			

[a] n = number of samples used in the calibration or validation sets, respectively. [b] Independent validation set. [c] r = correlation coefficient. [d] PLS factors = number of factors used to develop the calibration model.

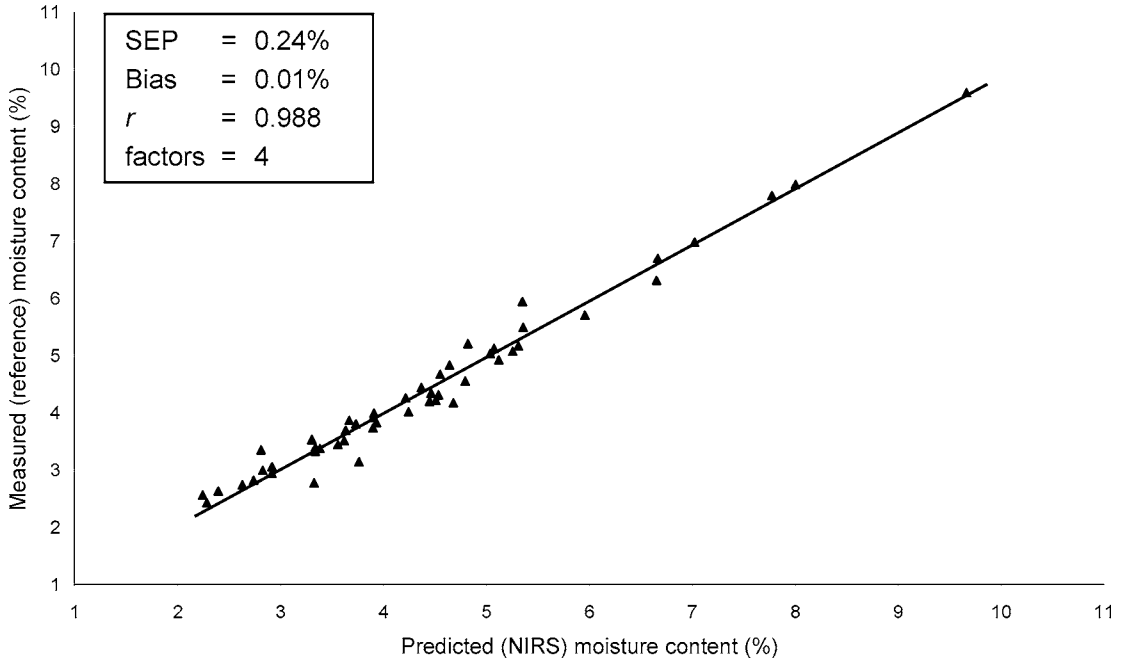

Figure 5. Scatter plot of the validation samples ($n = 50$) for the FT-NIR moisture content calibration model of dried, ground devil's claw root. Measured (reference) values are plotted against predicted (NIRS) values.

of possible enzymatic degradation reactions in the presence of free water. Furthermore, the sample temperature remained low enough so as not to increase the reaction rate of any chemical degradation dramatically.

It is probable that the slow drying at 40 °C created a more ideal environment, with high enough water activity for enzymatic reactions to occur, than at either 50 or 60 °C, resulting subsequently in the lowest HS content. During the initial stages of drying, the sample temperature would remain lower than the T_{DB} (i.e., closer to the T_{WB}) and within the optimum range (ca. 25−35 °C) for enzyme activity. The lower HS content at 60 °C than at 50 °C could be due to the enhancement of temperature-dependent, nonenzymatic chemical reactions. Polymerization reactions with free amino acids may lead to the production of other intermediates that can possibly cause the reduction of HS content (*3*, *26*). The change in HS retention with drying temperature also indicated that the observed differences in drying rates are important.

NIRS Calibration Development. A summary of the reference data for moisture, HS, and 8ρCHG contents of the ground, dried devil's claw root is given in **Table 3**.

Moisture Content. The distribution of moisture content of the sample set is shown in **Figure 4**. The moisture content calibration consisted of 100 samples in the calibration set (range: 2.44−10.43%) and the remaining 50 in the independent validation set (range: 2.53−9.60%) (**Table 4**). For this particular calibration, preprocessing involved the use of Savitzky−Golay 1st derivative (segment size = 5) after MSC was applied to the spectra. The moisture content of devil's claw samples could be successfully predicted by NIRS analysis. The SEP for the moisture content calibration was determined as 0.24% (**Table 4**), and this value compared acceptably well with the SEL of 0.14% (**Table 3**). Furthermore, a small bias of 0.01% and an excellent correlation coefficient (r) of 0.988 were also observed (**Figure 5**). The RPD of 6.58 confirmed that the accuracy of the calibration model is adequate for it to be used during quality control. The performance of this model compared adequately to NIRS moisture calibrations on ground wheat samples with SEP values of 0.15 (range: 8.55−12.70%) (*29*) and 0.19% (12.5−14.7%) (*30*). Even though these values appear to be much lower than for the current study, the better performances of the wheat calibrations can partially be attributed to smaller moisture content ranges used.

From a quality control perspective, the rapid prediction of moisture content in dried devil's claw root is paramount to the storage stability of the product. Microbial spoilage that could

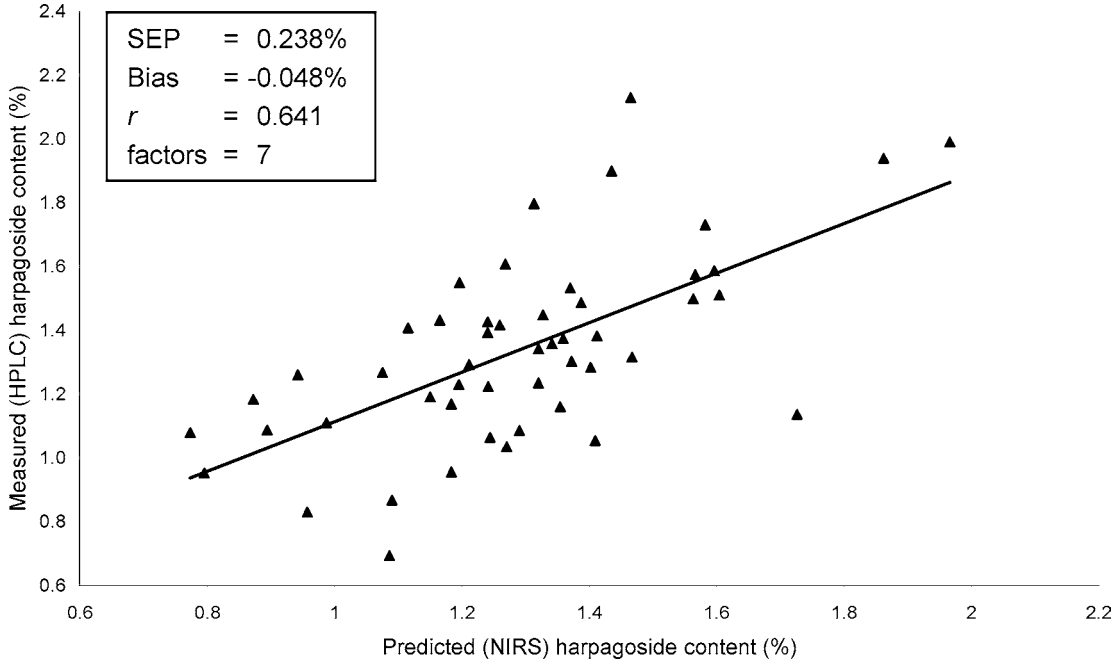

Figure 6. Scatter plot for the validation samples ($n = 50$) for the FT-NIR HS content calibration model. Reference HS values (determined by HPLC) are plotted against predicted NIRS HS values.

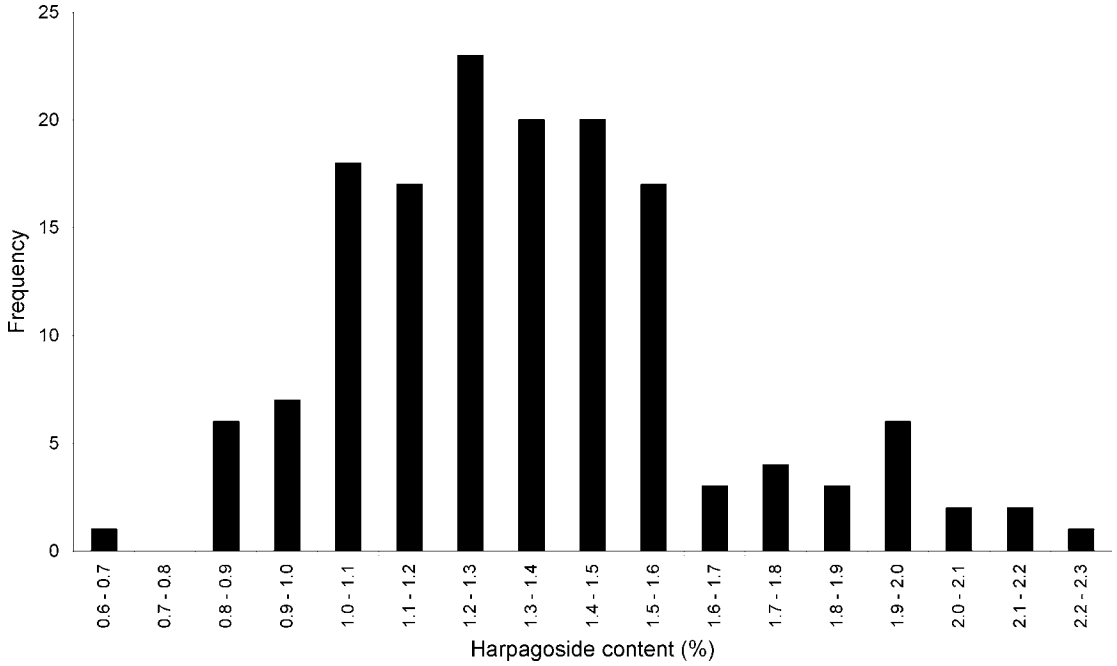

Figure 7. Histogram of the distribution of HS content between samples of dried, ground devil's claw root ($n = 150$).

possibly be detrimental to the HS content or could result in the formation of mycotoxins would occur rapidly if the moisture content was too high. Prediction of the moisture content by NIRS methods would assist in ensuring the export quality of this indigenous product.

HS Content. The best performance for the HS model resulted from the 1st derivative (Savitzky−Golay, segment size = 11)-treated data after MSC correction was applied. The NIRS HS model had an SEP of 0.236%, a bias of −0.048%, and an r of 0.641 (**Table 4** and **Figure 6**). A total of seven PLS factors were used. The SEP did not compare well with the calculated SEL of 0.035% (**Table 3**), but the NIRS model was not expected to be as sensitive as the HPLC reference method. Prediction with this NIRS model should therefore not be used for quantitative purposes but rather for screening to confirm the presence of HS in the root and to classify the product into specified ranges (semiquantitative measurements). This is also indicated by the RPD of 1.27. Slight improvement in the prediction accuracy for HS content (SEP = 0.195%) in devil's claw has recently been demonstrated with NIR-FT-Raman spectroscopy (*15*).

The main reason for the relatively poor prediction by FT-NIR is that the HS content range in this sample set is limited. The HS range also shows a near-Gaussian distribution (**Figure 7**) due to the randomness with which sample selection and preparation had occurred. This type of distribution will produce accurate estimations of HS close to the sample mean (ca. 1.4%) but less accurate results for samples near the extremes of the

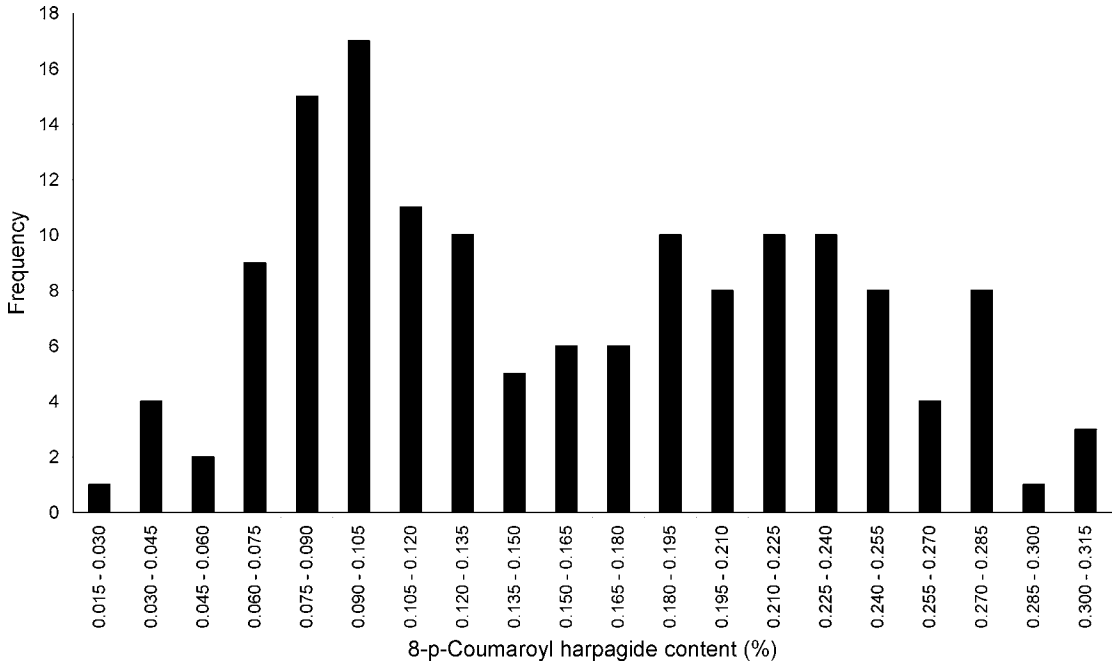

Figure 8. Histogram of the distribution of 8ρCHG content between samples of dried, ground devil's claw root ($n = 150$).

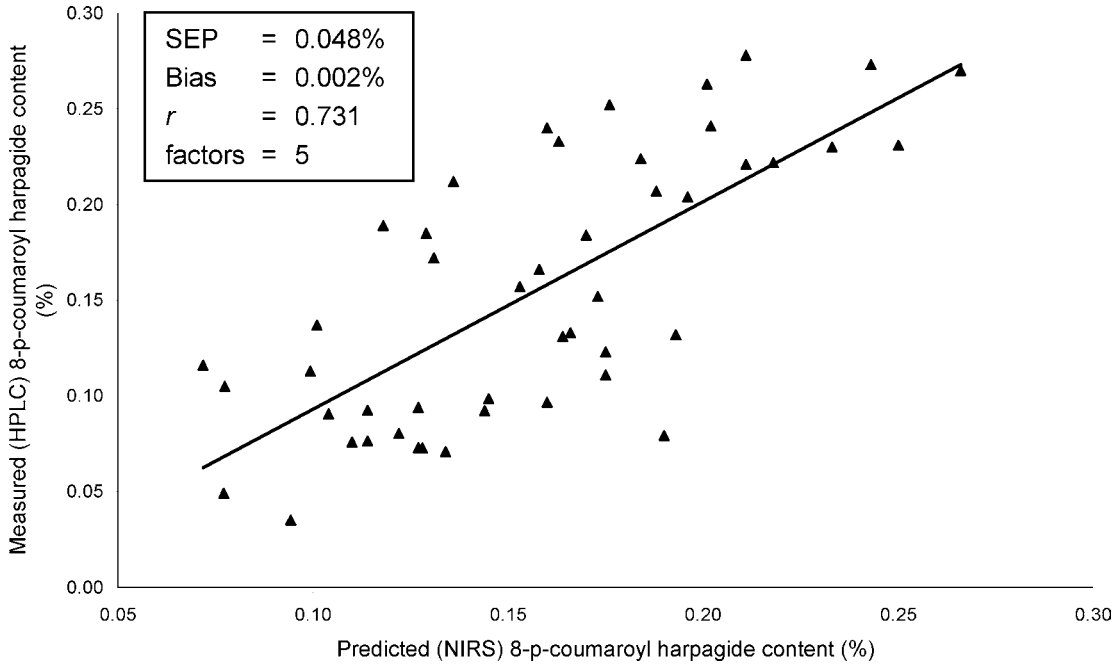

Figure 9. Scatter plot of the validation samples ($n = 50$) for the FT-NIR 8ρCHG content calibration model. Reference 8ρCHG values (determined by HPLC) are plotted against predicted NIRS 8ρCHG values.

range (*31*). Although any future samples are also likely to have a Gaussian distribution, the robustness and accuracy of the HS model would best be increased if sample selection had created an even distribution. The results of this study also showed promise for the use of NIRS technology as a classification tool for the medicinal potency of devil's claw as linked to its HS content. Although it is suggested that a suitable minimum level of 1.2% HS be enforced for standardization of the roots, there is a need for further classification. It would be advantageous if dried devil's claw samples could be classified as having HS contents of <1.2, between 1.2 and 1.6, between 1.6 and 2.5, or >2.5% for specific markets and premium priced roots.

8-ρ-Coumaroyl Harpagide Content. A histogram of the distribution of 8ρCHG content between samples of dried, ground devil's claw root is shown in **Figure 8**, and the samples showed a more even distribution of 8ρCHG than for HS content. An even distribution facilitates the development of accurate NIR models across a larger range of the estimated analyte (*31*). The best NIRS model had a SEP of 0.048%, a bias of 0.002%, an *r* of 0.731, and a RPD of 1.52, which indicate that the calibration model is also adequate for screening purposes (**Table 4** and **Figure 9**).

Loading Plots. Typical spectra of *H. procumbens* root are shown in **Figure 10**. After exclusion of particle size variation by MSC and application of the Savitzky−Golay 1st derivative, the largest remaining contributor to spectral variability is moisture content. The plot of the weights against wavelengths (loadings) for the first three principle components (PCs) shows

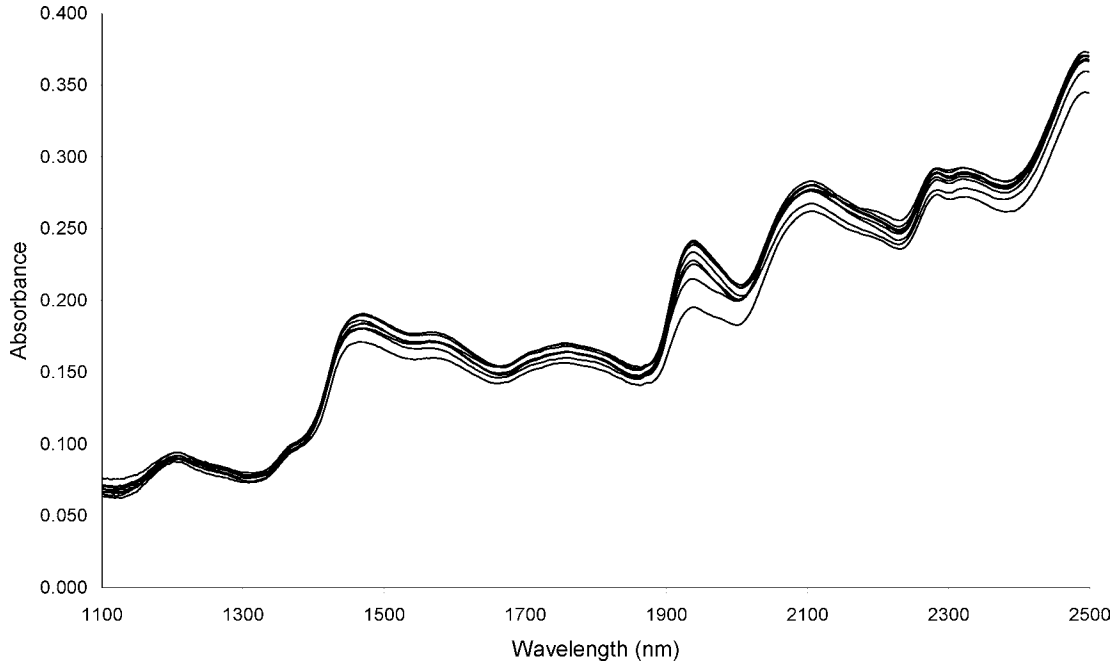

Figure 10. Typical NIRS spectra of dried, ground *H. procumbens* root.

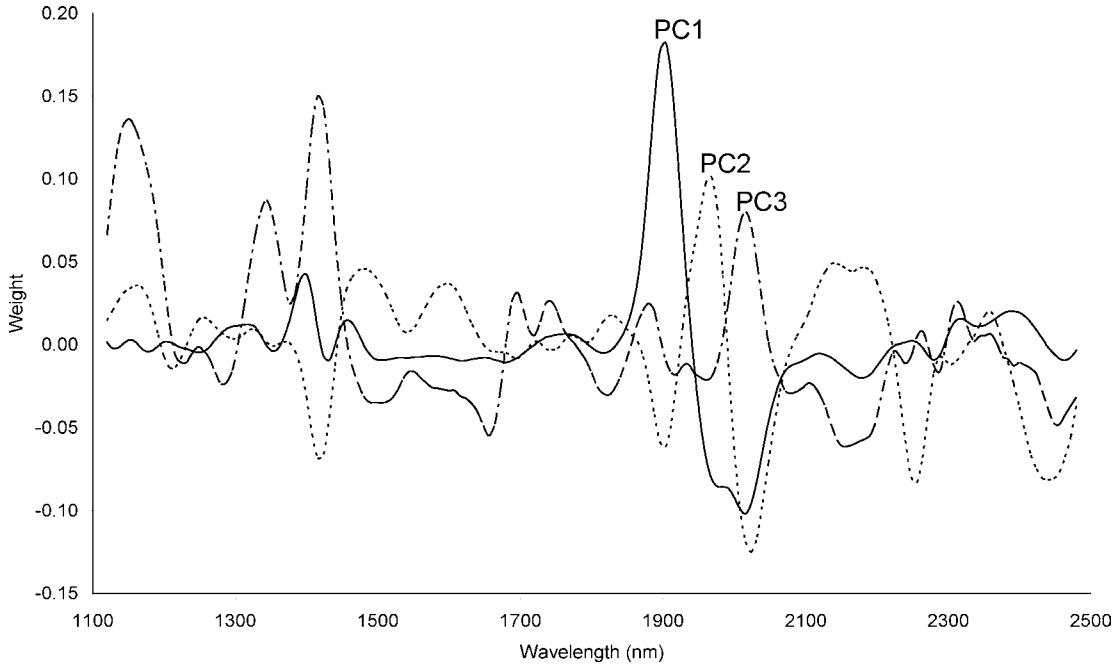

Figure 11. Plot of weights against wavelengths (loadings) for the first three PCs of dried, ground devil's claw root.

strong absorption at ca. 1400 nm (O−H stretch 1st overtone) and 1900 nm (O−H stretch + O−H deformation) (**Figure 11**). These wavelength regions correspond most strongly to the absorption of water, indicating that most of the information about moisture content is contained in the 1st PC (PC1). Similarly, most of the information about HS and 8ρCHG seems to be contained in the 2nd and 3rd PCs as shown by strong absorption at ca. 1968 (C═O stretch 2nd overtone), 2144 (═C−H stretch + C═C stretch), and 2192 (CH_2 asymmetrical stretch + C═ stretch) nm in PC2. These bonds are present in HS and 8ρCHG (**Figure 1**). Strong absorption is also shown in PC3 at ca. 2016 (2 × O−H deformation + C−O deformation), 1416 (2 × C−H stretch + C−H deformation), and 1344 (2 × C−H stretch + C−H deformation) nm. As expected, the relative contribution of the first three PCs to the spectral variability is large with 87, 6, and 4% explained by PC1, PC2, and PC3, respectively.

Sun drying of devil's claw root is detrimental to the retention of HS, and tunnel drying provides a means of improving HS retention. NIR analysis may provide a rapid and easily used method to quantify moisture content and screen devil's claw root for minimum HS levels during quality control.

ABBREVIATIONS USED

8ρCHG, 8-ρ-coumaroyl harpagide; FT-NIR, Fourier transform near-infrared; HDPE, high-density polyethylene; HPLC, high-performance liquid chromatography; HS, harpagoside; ICRA, IdentiCheck reflectance accessory; MSC, multiplicative scatter correction; NIR, near-infrared; NIRS, near-infrared spectroscopy; *r*, correlation coefficient; PC, principle component; PLS,

partial least squares regression; RH, relative humidity; RMSEP, root-mean-square error of prediction; SEL, standard error of laboratory; SEP, standard error of prediction; SD, standard deviation; T_{DB}, dry bulb temperature; T_{WB}, wet bulb temperature.

ACKNOWLEDGMENT

We thank Gerard Hansford for kindly supplying the fresh devil's claw root and for sharing his expertise and knowledge as well as the technical assistance of personnel of the Post-Harvest & Wine Technology Division of ARC Infruitec-Nietvoorbij. We also thank Dr. Chris Hansmann for the use of the drying tunnels and expert advice.

LITERATURE CITED

(1) Watt, J. M.; Breyer-Brandwijk, M. G. *The Medicinal and Poisonous Plants of Southern and Eastern Africa*, 2nd ed.; E & S Livingstone Ltd.: London, United Kingdom, 1962; pp 1−830.

(2) Eichler, O.; Koch, C. Über die antiphlogistische, analgetische und spasmolytische Wirksamkeit von Harpagosid, einem Glykosid aus der Wurzel von *Harpagophytum procumbens* DC. *Arzneim.-Forsch.* **1970**, *20*, 107−109.

(3) Baghdikian, B.; Lanhers, M.-C.; Fleurentin, J.; Ollivier, E.; Maillard, C.; Balansard, G.; Mortier, F. An analytical study, antiinflammatory and analgesic effects of *Harpagophytum procumbens* and *Harpagophytum zeyheri*. *Planta Med.* **1997**, *63*, 171−176.

(4) George, J.; Laing, M. D.; Drewes, S. E. Phytochemical research in South Africa. *S. Afr. J. Sci.* **2001**, *97*, 93−105.

(5) Czygan, F.-C.; Krüger, A. Pharmazeutisch-biologische untersuchungen der gattung *Harpagophytum* 3. Mitteilung: Zur verteilung des iridoid-glucosids harpagosid in den einzelnen organen von *Harpagophytum procumbens* DC und *Harpagophytum zeyheri* DECNE. *Planta Med.* **1977**, *31*, 305−307.

(6) Eich, J.; Schmidt, M.; Betti, G. HPLC analysis of iridoid compounds of *Harpagophytum* taxa: Quality control of pharmaceutical drug material. *Pharmacol. Lett.* **1998**, *8* (4), 75−78.

(7) Chrubasik, S.; Sporer, F.; Dillmann-Marschner, R.; Friedmann, A.; Wink, M. Physicochemical properties of harpagoside and its *in vitro* release from *Harpagophytum procumbens* extract tablets. *Phytomedicine* **2000**, *6*, 469−473.

(8) Guillerault, L.; Ollivier, E.; Elias, R.; Balansard, G. Determination of harpagide, 8-para-coumaroyl harpagide and harpagoside by high performance liquid chromatography in *Harpagophytum procumbens* drugs and in a commercial extract. *J. Liq. Chromatogr.* **1994**, *17*, 2951−2960.

(9) Wu, H.; Chuang, W.; Sheu, S. Separation of nine iridoids by capillary electrophoresis and high-performance liquid chromatography. *J. Chromatogr. A* **1998**, *803*, 179−187.

(10) Poukens-Renwart, P.; Tits, M.; Angenot, L. Quantitative densitometric evaluation of harpagoside in the secondary roots of *Harpagophytum procumbens* DC. *J. Planar Chromatogr.—Mod. TLC* **1996**, *9*, 199−202.

(11) Feistel, B.; Gaedcke, F. Analytische Identifizierung von Radix Harpagophyti procumbentis und zeyheri. *Z. Phytotherapie* **2000**, *21*, 246−251.

(12) Ren, G.; Chen, F. Simultaneous quantification of ginsenosides in American ginseng (*Panax quinquefolium*) root powder by visible/near-infrared reflectance spectroscopy. *J. Agric. Food Chem.* **1999**, *47*, 2771−2775.

(13) Schulz, H.; Engelhardt, U. H.; Wegent, A.; Drews, H.-H.; Lapczynski, S. Application of near-infrared reflectance spectroscopy to the simultaneous prediction of alkaloids and phenolic substances in green tea leaves. *J. Agric. Food Chem.* **1999**, *47*, 5064−5067.

(14) Steuer, B.; Schulz, H.; Läger, E. Classification and analysis of citrus oils by NIR spectroscopy. *Food Chem.* **2000**, *72*, 113−117.

(15) Baranska, M.; Schulz, H.; Siuda, R.; Strehle, M. A.; Rösch, P.; Joubert, E.; Manley, M. Quality control of *Harpagophytum procumbens* and its related phyto-pharmaceutical products by means of NIR-FT-Raman spectroscopy. *Biopolymers* **2005**, *77*, 1−8.

(16) Huck, C. W. Advances in near-infrared spectroscopy in phytochemistry. In *Near Infrared Spectroscopy: Proceedings of the 10th International Conference*; Davies, A. M. C., Cho, R. K., Eds.; The Cromwell Press: Wiltshire, United Kingdom, 2002; pp 491−496.

(17) Burger, J. F. W. Nuwe inhoudstowwe van 'n medisinale plant, *Harpagophytum procumbens* DC. M.Sc. in Chemistry Thesis, University of the Free State, South Africa, 1985.

(18) Hansmann, C. F.; Van Noort, G. An experimental fruit dehydration system. *Drying Technol.* **1992**, *10*, 491−508.

(19) Naes, T.; Isaksson, T. The chemometric space: SEP or RMSEP, which is best? *NIR News* **1991**, *2* (4), 16.

(20) Lanhers, M.-C.; Fleurentin, J.; Mortier, F.; Vinche, A.; Younos, C. Antiinflammatory and analgesic effects of an aqueous extract of *Harpagophytum procumbens*. *Planta Med.* **1992**, *58*, 117−123.

(21) Hallström, B.; Skjöldebrand, C. Heat and mass transport in solid foods. In *Developments in Food Preservation*; Thorne, S., Ed.; Applied Science Publishers: London, United Kingdom, 1983; pp 61−94.

(22) Rockland, L. B.; Nishi, S. K. Influence of water activity on food product quality and stability. *Food Technol.* **1980**, *34* (4), 42−51.

(23) Conn, E. E. β-Glucosidases in plants: Substrate specificity. In *β-Glucosidases: Biochemistry and Molecular Biology*; Esen, A., Ed.; American Chemical Society: Washington, DC, 1993; pp 15−26.

(24) Vámos-Vigyázó, L. Prevention of enzymatic browning in fruits and vegetables—A review of principles and practice. In *Enzymatic Browning and Its Prevention*; Lee, C. Y., Whitaker, J. R., Eds.; American Chemical Society: Washington, DC, 1995; pp 49−59.

(25) Diamante, L. M.; Munro, P. A. Mathematical modelling of hot air-drying of sweet potato slices. *Int. J. Food Sci. Technol.* **1991**, *26*, 99−109.

(26) Ziller, K. H.; Franz, G. Analysis of the water soluble fraction from the roots of *Harpagophytum procumbens*. *Planta Med.* **1979**, *37*, 340−348.

(27) Von Loesecke, H. W. *Drying and Dehydration of Foods*; Reinhold Publishing Corporation: New York, 1945; pp 37, 81−117.

(28) Thijssen, H. A. C. Optimization of process conditions during drying with regard to quality factors. *Lebensm. Wiss. Technol.* **1979**, *12*, 308−317.

(29) Manley, M.; Van Zyl, L.; Osborne, B. G. Using Fourier transform near-infrared spectroscopy in determining kernel hardness, protein and moisture content of whole wheat flour. *JNIRS* **2002**, *10*, 71−76.

(30) Sorvaniemi, J.; Kinnunen, A.; Tsados, A.; Mälkki, Y. Using partial least squares regression and multiplicative scatter correction for FT-NIR data evaluation of wheat flours. *Lebensm. Wiss. Technol.* **1993**, *26*, 251−258.

(31) Osborne, B. G.; Fearn, T.; Hindle, P. H. *Practical NIR Spectroscopy with Applications in Food and Beverage Analysis*; Longman Scientific & Technical: London, United Kingdom, 1993; pp 1−227.

Received for review December 9, 2004. Revised manuscript received February 21, 2005. Accepted February 24, 2005.

JF047930C